Organic & Biomolecular Chemistry

RSC Publishing

PAPER

View Article Online
View Journal | View Issue



Cite this: *Org. Biomol. Chem.*, 2013, **11**, 7721

# Lighting up cysteine and homocysteine in sequence based on the kinetic difference of the cyclization/addition reaction†

Fuqiang Guo,‡[a] Minggang Tian,‡[a] Fang Miao,[a] Weijia Zhang,[a] Guofen Song,[a] Yong Liu,[a] Xiaoqiang Yu,*[a] Jing Zhi Sun*[b] and Wai-Yeung Wong*[c]

Received 9th July 2013,
Accepted 5th September 2013

DOI: 10.1039/c3ob41414k

www.rsc.org/obc

A novel one- and two-photon fluorescent probe **CB1** has been developed for discriminating Cys and Hcy in a successive manner with high selectivity. The discrete time-dependent fluorescent responses enable us to sequentially detect Cys and Hcy in different time windows. Two-step reaction and kinetic modes were used to explain the sensing mechanism. As a promising biosensor for cell imaging, **CB1** has been confirmed to exhibit membrane permeability to intact cells, low cytotoxicity to viable cells and photostability to ultraviolet light excitation. Furthermore, the results from the control assay have shown that the one- and two-photon fluorescence of **CB1** within cells is associated with intracellular mercapto biomolecules but yet there is little interference with physiological pH value, viscosity and common bioanalytes. Finally one- and two-photon fluorescent images of **CB1** within living SiHa cells have been presented.

## Introduction

Discriminative detection of analogous molecules in biological systems is of great significance. For example, cysteine (Cys) and homocysteine (Hcy) are homologues except that Hcy possesses an additional methylene on the side-chain. But Cys and Hcy play distinctive roles in a series of biological processes.[1,2] Cys is an indispensable amino acid in various proteins and peptides.[3–5] A high level of Cys is clinically relevant to rheumatoid arthritis,[6] Parkinson's disease,[7] Alzheimer's disease[7–9] and adverse pregnancy outcomes.[10] As for Hcy, the excess of Hcy has also been proved to be a risk factor for diabetes[11,12] and cardiovascular diseases.[13–15] Very importantly, a number of studies in the past decade indicate that Hcy is a graded, independent risk factor for myocardial infarction, stroke and venous thromboembolism.[16–19] Up to now, a few strategies such as high performance liquid chromatography,[20] gas chromatography-mass spectrometry,[21] capillary electrophoresis separations,[22] electro-chemical assays,[23] and plasmon enhancement based on the interaction between Au nanorods,[24] nanoparticles[25] and synthetic reporters[26] have been carried out for thiol detection. Among these techniques, the optical assay based on fluorescent probes has been extensively studied due to its advantages including high sensitivity, low cost, facile operation, visual signal transduction, real-time *in situ* responses, and suitability for *in vivo* analysis.

However, it is a challenging task to discriminatively detect Cys over Hcy or *vice versa* with fluorescent probes. The bottleneck is ascribed to the deficient molecular design of the fluorescent probes. Cys and Hcy have identical reactive groups that can be used for chemical linking to fluorophores. Consequently, most fluorescent probes that have been developed so far can simultaneously react with both Cys and Hcy, and sometimes with other biomolecules containing thiol groups, such as glutathione (GSH) and *N*-acetyl-L-cysteine (NAC).[27–34] For example, since the pioneering work of Strongin and colleagues,[35] fluorophores bearing aldehydes and/or acrylates have been used as fluorescent probes for the detection of Cys and Hcy. Usually, this strategy allows the detection of the total content of Cys and Hcy because of the similar reactivity of the amino–thiol groups on Cys and Hcy with aldehydes.[36]

The mechanistic investigations indicated that the reaction between the aldehyde-functionalized fluorophore and Cys/Hcy is associated with the cyclization reaction of amino and thiol

[a]*Center of Bio & Micro/Nano Functional Materials, State Key Laboratory of Crystal Materials, Shandong University, Jinan, 250100, P. R. China. E-mail: yuxq@sdu.edu.cn; Fax: (+86)531-8836-6418*
[b]*MoE Key Laboratory of Macromolecule Synthesis and Functionalization, Institute of Biomedical Macromolecules, Department of Polymer Science and Engineering, Zhejiang University, Hangzhou, 310027, P. R. China. E-mail: sunjz@zju.edu.cn*
[c]*Institute of Molecular Functional Materials and Department of Chemistry and Institute of Advanced Materials, Hong Kong Baptist University, Waterloo Road, Hong Kong, P. R. China. E-mail: rwywong@hkbu.edu.hk*
†Electronic supplementary information (ESI) available. See DOI: 10.1039/c3ob41414k
‡Guo and Tian made equal contributions to this work.

groups with aldehydes to form thiazolidines/thiazinanes.[37–39] Cys may form generally more favored 5-/7-membered ring heterocycles upon reaction with aldehydes and acrylates, in comparison to the less favored 6-/8-membered ring heterocycles that result from Hcy. Due to the difference in activation energy, the cyclization reaction rate showed a difference. This difference has been used in the discriminative detection of Cys over Hcy and significant progress has been achieved. Representative work was reported by Strongin's group. They exploited the conjugate addition of Cys/Hcy to acrylates to generate thioethers, which can additionally undergo intramolecular cyclization to yield 7-/8-membered ring heterocycles. In kinetics, the formation of an 8-membered ring is disfavored relative to the formation of a 7-membered ring. Thus, by linking an α,β-unsaturated carbonyl moiety to 2-(2′-hydroxyphenyl) benzothiazole (HBT), a fluorescent probe for the discrimination of Cys and Hcy based on their different rates of intramolecular cyclization and the excited-state intramolecular photon-transfer process of HBT has been realized.[38] Similarly, the kinetic difference in the formation of differential-membered heterocycles by the reaction of Cys/Hcy with aldehydes has also been used to design fluorescent probes for the selective detection of Cys and Hcy. Lin and co-workers reported a ratiometric fluorescent probe constructed by attaching an α,β-unsaturated aldehyde moiety onto a coumarin fluorophore, which showed a specific fluorescent response to Cys over Hcy and GSH with evident distinction in the kinetic profiles.[39] Mei *et al.* modified tetraphenylethene (TPE) and silole-based fluorophores with two aldehydes.[40,41] The formation of thiazinane/thioazolidine led to aggregation of the fluorophores, which induced strong emission from the aggregates. The difference in reaction rates determined the appearance of aggregation-induced emission at different times for Cys and Hcy. Other thiols did not undergo the cyclization reaction, and thus did not interfere with the detection process.

In our previous work, we reported a fluorescent probe (**CA1**, Chart 1) for the discriminative detection of Cys over Hcy.[42] We also carried out the bioimaging experiments in living cells by using **CA1** as a fluorescent probe and the results indicated that the fluorescence turn-on probe showed high staining efficiency to living SiHa cells and good imaging contrast. Here, we report the amelioration to fluorescent probe **CA1**. The chemical structure of the new probe is shown in Chart 1 (**CB1**)§. We keep the basic structure of **CA1** unchanged in order to conserve the membrane permeability of the fluorescent probe into living cells. We will confirm that **CB1** is a promising biosensor for cell imaging with good membrane permeability and low cytotoxicity to intact cells. The bioimaging property has not been studied by Strongin and colleagues and Mei *et al.* in their work.[38,40,41] In addition, the insertion of an ethene group between the carbazole and aldehyde moieties would not evidently change the electronic structure of **CA1**. As a result, **CB1** should possess strong two-photon excited fluorescence (TPEF),

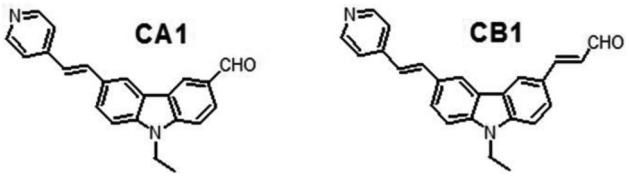


**Chart 1** Chemical structure of **CA1** and **CB1**.

which allows the bioimaging process to be inspected by two-photon microscopy (TPM), a technique that enjoys higher spatial resolution and lower photo-bleaching in comparison with the commonly used confocal microscopy technique. Up to now, only a few TPEF probes have been developed for the detection of Cys and Hcy.[36,42–44] More importantly, the replacement of a monoaldehyde on **CA1** by an α,β-unsaturated aldehyde moiety may bestow the derivative **CB1** with an amplified kinetic rate difference, which enables us to clearly discriminatively detect Cys over Hcy or *vice versa* in different time windows.

## Results and discussion

### Time dependent fluorescence responses of CB1 to Cys and Hcy

To examine the kinetic rate difference between the reactions of **CB1** with Cys and Hcy, we monitored the time-dependent changes of the fluorescence features of **CB1** upon the addition of Cys and Hcy in EtOH–PBS buffer solution, and the recorded data are shown in Fig. 1. **CB1** displays a very weak and broad fluorescence band with a peak at around 463 nm, and the fluorescence intensity has no measurable change with time-lapse. After adding Cys into the buffer solution, the fluorescence intensity of the mixture (**CB1** + Cys) is enhanced gradually. Meanwhile, the emission band becomes narrower and the emission peak ($I_{463}$) becomes more and more pronounced (Fig. 1A and S1†). $I_{463}$ reaches the maximum within 40 min and then the time-dependent fluorescence intensity curve levels off (Fig. 1A). By further extending the reaction time from 2 to 8 h, $I_{463}$ declines slightly. Then $I_{463}$ undergoes a fast decrease and the mixture becomes faintly emissive in about 16 h (Fig. 1B). The images showing the fluorescence changes are shown as the inset in Fig. 1B.

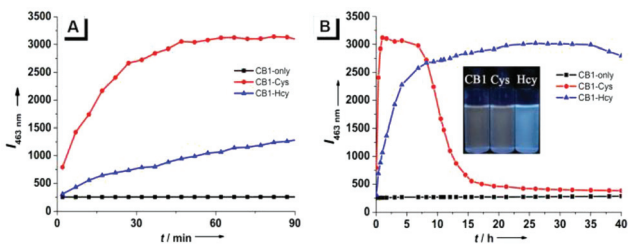


**Fig. 1** Time-dependent fluorescence intensity changes of **CB1** (10 μM) at $\lambda$ = 463 nm upon adding Cys and Hcy (600 μM) in EtOH–PBS buffer solution (v/v 4 : 1, 20 mM, pH 7.4) at room temperature. A: 0–90 min and B: 0–40 h, $\lambda_{ex}$ = 365 nm. Inset B: photos under UV light ($\lambda_{ex}$ = 365 nm), 40 h.

§ **CB1** is available free.

Under the same conditions, the addition of Hcy into **CB1** buffer solution can also result in changes of fluorescence features. But the **CB1** + Hcy system shows distinct time-dependent features in comparison with the **CB1** + Cys system. The fluorescence intensity of the **CB1** + Hcy system increases slowly in the earlier stage (0–40 min, Fig. 1B). After reaction for 2 h, the fluorescence intensity grows to its maximum for the **CB1** + Cys system, about 12 times higher than that recorded for **CB1**. But the fluorescence intensity for the **CB1** + Hcy system in 2 h grows only to half of its maximum. In about 10 h, the fluorescence intensity approaches the maximum, and the fluorescence is sustained for a long time and only a small decrease is recorded after 35 h. We also checked the changes in UV-visible spectral features for the reaction mixtures of **CB1** with Cys and **CB1** with Hcy, but little changes were observed (Fig. S2A and S2B†).

### Mechanistic investigation

The different time-dependent fluorescence responses of **CB1** to Cys and Hcy suggest that the reactions of **CB1** with Cys and **CB1** with Hcy undergo different kinetic processes. Based on the literature results[37–39] and our previous investigations,[40–42] we propose a tentative mechanistic explanation as illustrated in Scheme 1. The thiol and amino groups on Cys attack the α,β-vinyl and the aldehyde groups on **CB1**, respectively, and a **CB1**–Cys adduct of a 7-membered ring heterocycle with a Schiff base structure is generated. In the neutral buffer solution, the **CB1**–Cys adduct has different isomers. The zwitterionic isomer **A** is the component that contributes to the recorded fluorescence, because the protonation of the pyridinyl moiety has altered the electronic structure of **CB1** and made the resulting product efficiently emissive. The formation of a 7-membered ring heterocycle is not as favourable as that of 5- and 6-membered rings, and thus the reaction of **CB1** with Cys is not as quick as that observed for the reactions of **CA1** with Cys[42] and aldehyde-functionalized tetraphenylethene with Cys.[40,41]

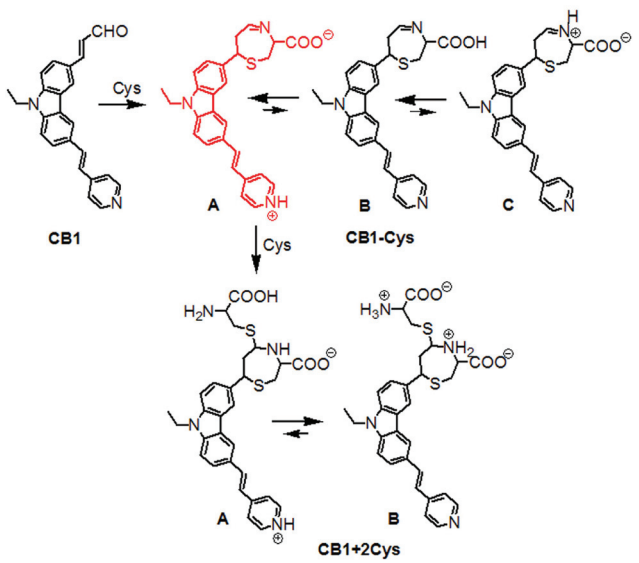


**Scheme 1** Proposed mechanism for the reaction between **CB1** and Cys.

The **CB1**–Cys adduct is an intermediate, which can react with the excess Cys through the addition of the residual thiol to the Schiff base in the 7-membered heterocycle. As a result, a new adduct of **CB1**–2Cys is produced. Upon this addition reaction, a secondary amine is transformed from the Schiff base and it is a stronger base that can seize the proton from the pyridyl moiety. Consequently, the fluorescence from the isomer **A** of the **CB1**–Cys adduct is quenched, just as displayed in Fig. 1.

It should be noted that the concentration of Cys (600 μM) is much higher than that of **CB1** (10 μM) as well as the **CB1**–Cys adduct. The second addition reaction must be a slower step. Otherwise, the **CB1**–Cys adduct generated from the first addition would be quickly consumed by the second addition; thereby no fluorescence enhancement could be observed. In fact, the addition of thiol to the C=N double bond in Schiff base is much slower than the thiol–ene addition between thiol and the C=C double bond that is activated by aldehyde or carboxylic ester and anhydride groups.[45] Reasonably, the accumulation of the **CB1**–Cys adduct by the first addition of the thiol of Cys to the α,β-unsaturated aldehyde moiety of **CB1** exceeds its consumption by the second addition of the thiol of Cys to the Schiff base. Therefore, the fluorescence is enhanced gradually with the accumulation of the **CB1**–Cys adduct. When **CB1** has been largely reacted, the consumption rate is lower than the accumulation one and the fluorescence intensity reaches the maximum. Then, the consumption has a pronounced effect, and the fluorescence intensity begins to decline. Once **CB1** has been completely consumed, the fluorescence intensity decreases quickly. As a direct proof, Fig. 1B demonstrates that the rate of fluorescence quenching is slower than that of fluorescence ascending.

To clarify the mechanism, the presence of the intermediate of the **CB1**–Cys adduct should be identified. Based on our experimental results, most of the **CB1** has been converted to the intermediate and the intermediate has been partially consumed by the second addition reaction at 2 h in the time course. We analyzed the reaction system at 2 h by utilizing high resolution mass spectroscopy (HRMS) and $^1$H NMR spectroscopy. The data of HRMS clearly show two pronounced peaks at *m*/*z* values of 456.1746 and 577.1961 (Fig. S3A†), which can be precisely assigned to **CB1**–Cys + $H^+$ and **CB1**–2Cys + $H^+$, respectively. We further examined the resulting mixture with HRMS at 24 h, where the **CB1** and **CB1**–Cys components are assumed to be completely consumed. As expected, the spectrum only shows a single peak at 577.1920 (Fig. S3B†), indicating the sole presence of **CB1**–2Cys. Moreover, $^1$H NMR spectroscopic characterization provides further evidence. As shown in Fig. S4A,† the signals corresponding to $\delta$ = 9.69 and $\delta$ = 6.89 ppm are assigned to the aldehyde protons (marked as $H^a$) and double-bond (marked as $H^b$, $J$ = 15.72 Hz) of **CB1**. After reaction for 2 h, the peaks of these two protons are much weakened. Meanwhile, two new multiplet-peaks (marked as $H^c$, $\delta$ = 5.35 ppm) appear and they can be assigned to the

proton on the carbon atom of the Schiff base moiety in the 7-membered ring (Fig. S4B†). As the reaction time was prolonged to 24 h, peaks of $H^c$ completely disappeared (Fig. S4C†), which could be associated with the second addition of Cys to the **CB1**–Cys adduct, which changes the chemical shift of $H^c$ to a high-field position ($\delta$ < 5.35 ppm). Therefore, both HRMS and $^1$H NMR data indicate the presence of **CB1**–Cys and **CB1**–2Cys adducts.

Another key point in the proposed mechanism is the presence of the equilibrium between the isomers. Assuming that isomer **A** is the fluorescent species, the removal of the proton on the pyridyl moiety will decrease the fluorescence intensity. We compared the fluorescent behavior of the **CB1** + Cys system at different pH values after reaction for 2 h, and the results are shown in Fig. S5A.† As expected, the fluorescence intensity of the mixture descends monotonously with the increase of pH value from 7 to 9. Rationally, ascending the acidity should increase the fluorescence intensity. But it leads to an evident decrease of the fluorescence intensity by further decreasing the pH to 4 (Fig. S5A†). This observation can be explained by the fact that the Schiff base is unstable in acidic aqueous solutions. At pH 4, the formation of the **CB1**–Cys adduct is greatly retarded. As a result, the fluorescence enhancement is not apparent.

As for the **CB1** + Hcy system, the reaction mechanism is similar to that described for the **CB1** + Cys system, except for the difference in the reaction kinetic rates. Scheme S1† illustrates the proposed reaction route. By adding a methylene unit to the residual part of Cys, the formation of an 8-membered ring becomes more disfavoured, and the reaction of **CB1** with Hcy is much slower than that of **CB1** with Cys. Based on the time course shown by Fig. 1B, we used the HRMS technique to analyze the resultants of the **CB1** + Hcy system after reaction for 24 and 36 h. The mass spectra show that the peak at *m*/*z* 470.1889 is stronger while the peak at *m*/*z* 605.2227 is rather weak (Fig. S6A and S6B†). The $^1$H NMR spectra at 24 and 36 h of this system are shown in the ESI.† At 24 h, the $^1$H NMR spectrum of the reaction system resembles that of Cys at 2 h: $H^a$ of aldehyde and $H^b$ of the C=C double bond become weaker, while $H^c$ of the C=N double bond on an 8-membered ring appears (Fig. S7A†). It is noticeable that $H^c$ still exists after reaction for 96 h (Fig. S7B†), indicating the slowness of the addition of the second Hcy to the **CB1**–Hcy adduct.

### Sequential detection of Cys and Hcy, selectivity and sensitivity

According to the experimental data and the proposed detection mechanism, we chose 40 min and 24 h as two time windows to inspect the feasibility of sequentially detecting Cys and Hcy by using **CB1** as the fluorescent probe. The experimental data are shown in Fig. 2. At 40 min, free **CB1** is faintly fluorescent, while the **CB1** + Cys system is highly fluorescent and a sharp contrast can be seen from the emission images shown by the inset of Fig. 2A. In the same time span, the **CB1** + Hcy system is still weakly fluorescent. Comparing the fluorescence intensity at the emission peak ($I_{463}$) of **CB1**, **CB1** + Cys and **CB1** + Hcy, the relative $I_{463}$ values are 1, 14.1 and 3.7, respectively. After reaction for 24 h, the data changed markedly. The relative $I_{463}$ values are 1, 2.2 and 14.5 for **CB1**, **CB1** +

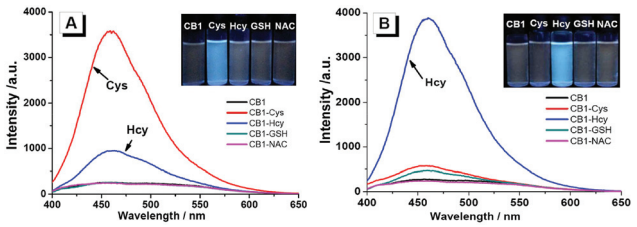


**Fig. 2** SPEF of **CB1** only and its mixtures with Cys, Hcy, GSH, NAC in EtOH–PBS buffer solution (v/v 4 : 1, 20 mM, pH 7.4) at room temperature. Concentration, [**CB1**] = 10 μM, [Cys] = [Hcy] = [GSH] = [NAC] = 600 μM. $\lambda_{ex}$ = 365 nm. Action time: A 40 min and B 24 h. Inset: photos under UV light ($\lambda_{ex}$ = 365 nm), A: 40 min and B: 24 h.

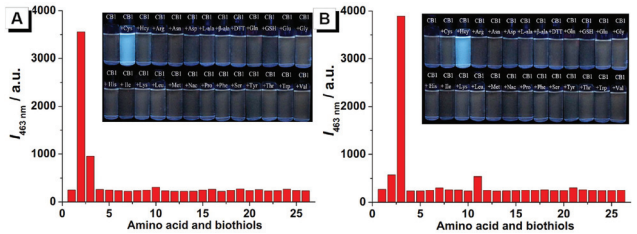


**Fig. 3** SPEF of **CB1** (10 μM) to various bioanalytes (600 μM) in EtOH–PBS buffer solution (v/v 4 : 1, 20 mM, pH 7.4) at room temperature. From left to right: 1-Blank, 2-Cys, 3-Hcy, 4-Arg, 5-Asn, 6-Asp, 7-L-Ala, 8-β-Ala, 9-DTT, 10-Gln, 11-GSH, 12-Glu, 13-Gly, 14-His, 15-Ile, 16-Lys, 17-Leu, 18-Met, 19-NAC, 20-Pro, 21-Phe, 22-Ser, 23-Tyr, 24-Thr, 25-Trp, 26-Val. $\lambda_{ex}$ = 365 nm. Action time: A, 40 min and B, 24 h. Inset: photos under UV light ($\lambda_{ex}$ = 365 nm), A: 40 min and B: 24 h.

Cys and **CB1** + Hcy, respectively (Fig. 2B). The discrete time-dependent fluorescent responses enable us to sequentially detect Cys and Hcy in different time windows.

The selectivity of a probe is of fundamental importance for its practical application. Considering that other intracellular mercapto biomolecules may interfere with the detection of Cys and Hcy in bioassay application, we also checked the fluorescence responses of **CB1** to GSH, the most plentiful mercapto biomolecule in living cells, as well as to the protected Cys, or NAC. The results are also shown in Fig. 2A and 2B. It is clear that GSH and NAC have little interference with the detection processes at both time windows. The fluorescent images offer visual inspections (insets of Fig. 2A and 2B). In addition to GSH and NAC, the responses of **CB1** to various amino acids other than Cys and Hcy were examined under the same detecting condition as Cys and Hcy, and the obtained results are displayed in Fig. 3A and 3B, corresponding to reaction for 40 min and 24 h, respectively. All these results indicate that, with the aid of two clear-cut time windows, we can sequentially detect Cys and Hcy with high selectivity and low interference by the fluorescent responses to **CB1**.

In addition to selectivity, sensitivity is another crucial parameter of a fluorescent probe. We evaluated the sensitivity of **CB1** to Cys and Hcy in the defined buffer solutions with fluorescent spectroscopic titration experiments. 40 min and 24 h were selected as the time windows for the detection of Cys and Hcy, respectively. The changes in fluorescence intensity at

 

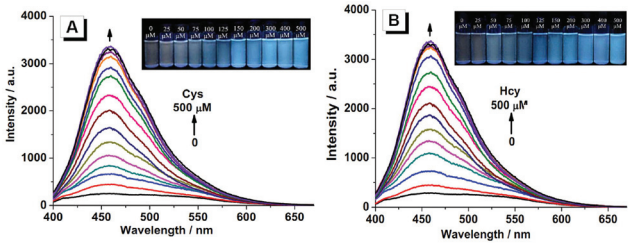


**Fig. 4** SPEF spectral changes of **CB1** (10 μM) upon addition of Cys and Hcy (0–500 μM) were recorded at 40 min and 24 h in EtOH–PBS buffer solution (v/v 4 : 1, 20 mM, pH 7.4) at room temperature. $\lambda_{ex}$ = 365 nm. Action time: A 40 min and B 24 h. Insets A and B: the photos of **CB1** in the presence of Cys (40 min) and Hcy (24 h) with various concentrations (from left to right: 0 μM, 25 μM, 50 μM, 75 μM, 100 μM, 125 μM, 150 μM, 200 μM, 300 μM, 400 μM, 500 μM) under UV light ($\lambda_{ex}$ = 365 nm).

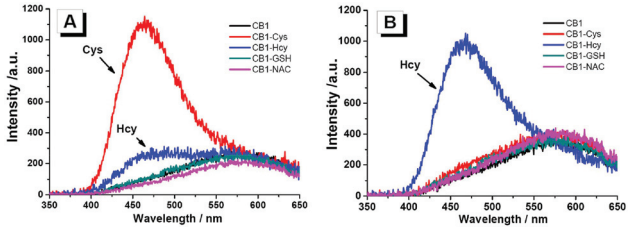


**Fig. 5** TPEF of **CB1** only and its mixtures with Cys, Hcy, GSH, NAC in EtOH–PBS buffer solution (v/v 4 : 1, 20 mM, pH 7.4) at room temperature. Concentration, [**CB1**] = 10 μM, [Cys] = [Hcy] = [GSH] = [NAC] = 600 μM. $\lambda_{ex}$ = 760 nm. Action time: A, 40 min and B, 24 h.

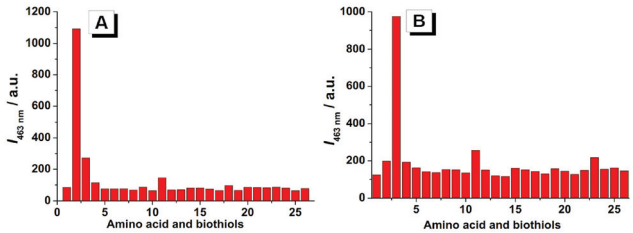


**Fig. 6** TPEF of **CB1** (10 μM) to various bioanalytes (600 μM) in EtOH–PBS buffer solution (v/v 4 : 1, 20 mM, pH 7.4) at room temperature. $\lambda_{ex}$ = 760 nm. Action time: A, 40 min and B, 24 h. All the bioanalytes are the same as Fig. 3.

463 nm ($I_{463}$) with Cys concentration in the defined medium are shown in Fig. 4A. $I_{463}$ increases linearly with the variation of Cys concentration from 0 to 300 μM. By further increasing the Cys concentration from 300 to 500 μM, the fluorescent titration curve levels off. According to work by Lin *et al.* and our previous work, intracellular Cys/Hcy could be detected when the corresponding fluorescence intensity is more than 3 times as strong as that of the probe only.[39,42] Thus, fluorescent responses were linearly fitted in a concentration range of Cys from 0 to 300 μM and a regression equation was obtained. Setting the fluorescent intensity to 3 times as strong as that of **CB1** only, the detection limit of Cys was calculated to be 59.8 μM according to the equation (Fig. S8†). Similarly, the detection limit of Hcy by **CB1** was calculated to be 58.6 μM (Fig. 4B and S9†).

### Two-photon excited fluorescence (TPEF) properties

An essential aim of the transformation of the fluorescent probe from **CA1** to **CB1** is to make use of the TPFE property of the **CA1** backbone. The TPFE technique enjoys the advantages of low photo-injury to living entities, large penetration depth, and high spatial resolution; thus it is a better technique than confocal microscopy in imaging living specimens.[46–48] Various TPEF probes have been investigated intensively and extensively by many researchers.[49–51] However, so far, there are only a few known TPEF sensors for detecting the total amount of Cys and Hcy,[36,42–44] including our reported TPEF probe of **CA1**.[42]

To confirm the transformation of CA1 to **CB1**, we investigated the TPEF performance of **CB1** in all aspects according to the conventional single-photon excited fluorescence (SPEF). Firstly, the TPEF behavior of **CB1** itself and the TPEF responses of **CB1** to four mercapto biomolecules (Cys, Hcy, GSH and NAC) have been examined in the same procedures as the measurements for SPEF. The results are displayed in Fig. 5A and 5B. The TPEF peak of free **CB1** appears at 583 nm and its intensity is rather low (Fig. 5A). In the time window of 40 min, the TPEF intensity of **CB1** + Cys obviously increases accompanied by a blue-shift of the emission peak from 583 to 463 nm. The TPEF of **CB1** + Hcy also blue-shifts to 463 nm from 583 nm, but the intensity is not enhanced. Similar to the observation in the case of SPEF, GSH and NAC do not interfere with the TPEF behavior of **CB1**. Quantitatively, the fluorescence intensity of **CB1** + Cys is 4.3 and 11.4 times as strong as that of **CB1** + Hcy and free **CB1**, respectively. In the time window of 24 h, the TPEF response of **CB1** to Hcy increases obviously and a blue-shift of the emission peak from 583 to 463 nm is also recorded (Fig. 5B). The fluorescence intensity of **CB1** + Hcy is 5.1 and 8.2 times as strong as that of **CB1** + Cys and free **CB1**, respectively. The results indicate that both GSH and NAC have a negligible effect on the emission property of **CB1**.

The TPEF responses of **CB1** to other different bioanalytes in the time windows of 40 min and 24 h are given in Fig. 6. The results show that TPEF responses of **CB1** to Cys are markedly higher than those to Hcy and other bioanalytes at 40 min (Fig. 6A), while at 24 h the TPEF responses of **CB1** to Hcy are much higher than those to bioanalytes including Cys, GSH and NAC (Fig. 6B). The sensitivity of the TPEF responses of **CB1** to Cys and Hcy has also been studied. The two-photon fluorescence titrations were carried out in the defined buffer solution within the two preset time windows. The fluorescent intensity at $\lambda$ = 463 nm ($I_{463}$) linearly increases on changing the concentration of Cys or Hcy from 0 to 300 μM (Fig. 7A and 7B). When the concentration of Cys or Hcy is higher than 300 μM, the intensity remains unchanged. The calculated detection limits for Cys and Hcy by the TPEF technique are 3.2 and 4.8 μM respectively, much lower than the intracellular concentrations of Cys (30–200 μM)[52] and Hcy (5–15 μM)[53] (Fig. S10 and S11†). To summarize the above experimental data, it is concluded that **CB1** can afford the highly discriminative and sensitive detection of Cys and Hcy by the TPEF technique.

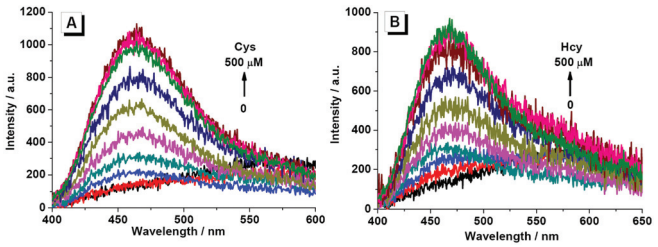


**Fig. 7** TPEF spectral changes of **CB1** (10 μM) upon addition of Cys and Hcy (0–500 μM) were recorded at 40 min (A) and 24 h (B) in EtOH–PBS buffer solution (v/v 4 : 1, 20 mM, pH 7.4) at room temperature. $\lambda_{ex}$ = 760 nm.

### Bioimaging for living cells

Combining the confirmed reaction mechanism, clear-cut time windows for Cys and Hcy detection, good TPEF property, and high selectivity for a target over various native cellular species, **CB1** seems to be an efficient fluorescent probe for bioimaging. Before using **CB1** to image living cells, we confirmed the excitation wavelengths of SPEF and TPEF for **CB1**, which are 365 and 760 nm respectively, corresponding to the working wavelength in wide-field and two-photon microscopes (TPM). Competition experiments were also performed, and addition of other bioanalytes did not result in the visible variation of SPEF and TPEF intensities of **CB1** + Cys at 40 min and **CB1** + Hcy at 24 h (Fig. S12†). In addition, at pH 4.0–8.0,[54] a wide physiological pH range representing an intracellular environment, the free **CB1** was weakly fluorescent, but **CB1** + Cys at 40 min and **CB1** + Hcy at 24 h exhibit high fluorescence intensity under neutral cytosol physiological conditions (pH 6.8–7.4)[55] (Fig. S5†). Then, we checked the effect of environmental viscosity on the fluorescent behavior of **CB1**. Commonly, the viscosity of cytoplasm is 1 to 2 cp and that around the membrane system is about 140 cp.[56] Our experimental results indicate that the interference in a viscosity range from 1.005 to 219 cp, covering the intracellular viscosity range, is also negligible (Fig. S13†).

In succession, we evaluated the cytotoxicity of **CB1** in SiHa cells by the MTT assay. The cell viability assay data of SiHa cells treated with 1 μM **CB1** during different incubation times were quantified (Table S1†). SiHa cells showed nearly 100% viability for 1 h and 93% for 24 h. Thus, **CB1** could be considered a low-toxicity fluorescent probe. The photostability of **CB1** in the presence and absence of Cys and Hcy was also examined in time windows of 40 min and 24 h. Though a certain fluorescence decay was recorded in the first 10 min, the fluorescence intensity of the **CB1**, **CB1** + Cys and **CB1** + Hcy systems can be sustained for more than 90 min, indicating the high photostability of **CB1** and its adducts with Cys and Hcy (Fig. S14–S16†).

Relying on the above preliminary experiments, we incubated living SiHa cells with **CB1** (1 μM) for 40 min and 24 h, and the differential interference contrast (DIC) images confirmed that the cells were viable throughout the imaging experiments.[57] SPEF and TPEF images were taken on the instruments of the wide-field and two-photon microscopes,

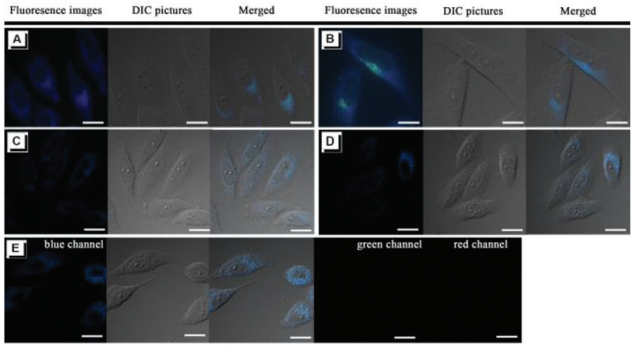


**Fig. 8** Images of **CB1** (1 μM) in SiHa cells with different incubation times. Wide field fluorescence images through the blue channel ($\lambda_{ex}$ = 330–385 nm; $\lambda_{em}$ > 410 nm). A: 40 min and B: 24 h; TPEF images ($\lambda_{ex}$ = 760 nm), C: 40 min and D: 24 h through the blue channel; E: TPEF images through three channels at 24 h: blue (430–460 nm), green (510–540 nm) and red (>565 nm). Bar = 20 μm.

and the recorded cell images are displayed in Fig. 8. As shown in Fig. 8A and 8B, fluorescent and merged photos demonstrated that intracellular parts emitted bright fluorescence and no fluorescence was observed in the extracellular regions. Therefore, **CB1** is a membrane-permeable probe. Furthermore, no fluorescence was found inside the nuclei, and the blue fluorescence existed only in certain parts of the cytoplasm. From Fig. 8C and 8D, TPEF imaging results are similar to that of SPEF, indicating **CB1** as a qualified TPEF probe as well. Fig. 8B and 8D give the images of cells that were incubated with **CB1** for 24 h, and the DIC images clearly show that the cells were still in good condition at that time.

To identify the source of intracellular emission, two strategies were used. We firstly designed a control experiment and the results are shown in Fig. S17.† Blank images without **CB1** at 40 min and 24 h show no detectable intracellular emission. When SiHa cells were pretreated with thio-blocking reagent *N*-ethylmaleimide (NEM) and then incubated with the probe, SPEF and TPEF in the cells almost disappeared at 40 min while becoming blurry at 24 h. Thus, intracellular fluorescence is undetectable without either **CB1** or biothiols. We also investigated the TPEF images at 24 h by means of three different channels, including a blue channel, a green channel and a red channel (Fig. 8E). As revealed by the fluorescent and merged images, bright fluorescence was found from the blue channel, while there was no emission from the green and red channels. Associated with experiments *in vitro*, the emission is believed to come from the reaction of **CB1** with biothiols.

## Conclusions

In summary, we report a novel one- and two-photon fluorescent probe **CB1** for discriminating Cys and Hcy in sequence with high selectivity. A two-step addition reaction mechanism has been confirmed by multiple spectroscopic characterizations and the mechanism can be used to reasonably explain the observed fluorescent behaviors of **CB1** and adducts of

 

**CB1**–Cys and **CB1**–Hcy. The amplified difference in kinetic rates allows the discriminative detection of Cys and Hcy in different time windows. Furthermore, probe **CB1** exhibits other advantages such as little interference with changes of pH value and viscosity, low cytotoxicity and high photostability. Intracellular imaging using both wide-field microscopy and TPM has been successfully achieved. Cell images through three different channels and thiol-blocking experiments confirmed the successful imaging of mercapto biomolecules in living cells. The discovery of **CB1** with these excellent properties offers a feasible strategy to design fluorescent probes for highly selective imaging of Hcy in living cells with both conventional confocal microscopy and advanced two-photon microscopy techniques.

## Acknowledgements

We thank NSFC 51273107, 51273175, ZR2012EMZ001, 2011JC006, SKLSSM201305, 2013CB834704, and the Research Grants Council of HKSAR (HKBU203011, HKUST2/CRF/10 and AoE/P-03/08) for financial support.

## Notes and references

1 J. Schulz, J. Lindenau, J. Seyfried and J. Dichgans, *Eur. J. Biochem.*, 2000, **267**, 4904.
2 Z. A. Wood, E. Schroder, J. R. Harris and L. B. Poole, *Trends Biochem. Sci.*, 2003, **28**, 32–40.
3 K. G. Reddie and K. S. Carroll, *Curr. Opin. Chem. Biol.*, 2008, **12**, 746.
4 E. Weerapana, C. Wang, G. M. Simon, F. Richter, S. Khare, M. B. D. Dillon, D. A. Bachovchin, K. Momen, D. Baker and B. F. Cravatt, *Nature*, 2010, **468**, 790.
5 R. Lill and U. Mühlenhoff, *Annu. Rev. Cell Dev. Biol.*, 2006, **22**, 457.
6 H. Bradley, A. Gough, R. S. Sokhi, A. Hassell, R. Waring and P. J. Emery, *Rheumatology*, 1994, **21**, 1192.
7 M. T. Heafield, S. Fearn, G. B. Steventon, R. H. Waring, A. C. Williams and S. G. Sturman, *Neurosci. Lett.*, 1990, **110**, 216–220.
8 G. S. Chai, X. Jiang, Z. F. Ni, A. J. Xie, X. S. Cheng, Q. Wang, J. Z. Wang and G. P. Liu, *J. Neurochem.*, 2013, **124**, 388.
9 L. El-Khairy, S. E. Vollset, H. Refsum and P. M. Ueland, *Am. J. Clin. Nutr.*, 2003, **77**, 467.
10 S. Patcharaporn, S. Surasak, S. Sorattaya, I. Siriwan, J. Sopida and K. Warangkana, *Diabetes Res. Clin. Pract.*, 2012, **98**, 151.
11 S. Badiou, A. M. Dupuy, I. Jaussent, A. Sultan, D. MarianoGoulart, J. P. Cristol and A. Avignon, *Clin. Chem. Lab. Med.*, 2012, **50**, 1099.
12 P. Sudchada, S. Saokaew, S. Sridetch, S. Incampa, S. Jaiyen and W. Khaithong, *Clin. Chem. Lab. Med.*, 2012, **50**, 1099.
13 P. M. Ueland and J. Loscalzo, *Clin. Chem.*, 2012, **58**, 1623.
14 F. Cacciapuoti, *Blood Coagul. Fibrin.*, 2012, **23**, 677.
15 K. Wustmann, M. Klaey, A. Burow and G. S. Shaw, *Cardiovasc. Ther.*, 2012, **30**, 277.
16 C. J. Boushey, S. A. Beresford, G. S. Omenn and A. G. Motulsky, *J. Am. Med. Assoc.*, 1995, **274**, 1049.
17 J. W. Eikelboom, E. Lonn, J. Genest Jr., G. Hankey and S. Yusuf, *Ann. Intern. Med.*, 1999, **13**, 363.
18 M. D. Heijer and M. B. A. Keijzer, *J. Clin. Chem. Lab. Med.*, 2001, **39**, 710.
19 S. R. Lentz and W. G. Haynes, *Cleveland Clin. J. Med.*, 2004, **71**, 729.
20 H. Refsum, A. D. Smith, P. M. Ueland, E. Nexo, R. Clarke, J. McPartlin, C. Johnston, F. Engbaek, J. Schneede, C. McPartlin and J. M. Scott, *Clin. Chem.*, 2004, **50**, 3.
21 A. Windelberg, O. Arseth, G. Kvalheim and P. M. Ueland, *Clin. Chem.*, 2009, **50**, 2103.
22 T. Inoue and J. R. Kirohhoff, *Anal. Chem.*, 2002, **74**, 1349.
23 W. Wang, L. Li, S. F. Li, C. P. Ma and S. S. Zhang, *J. Am. Chem. Soc.*, 2008, **130**, 10846.
24 P. K. Sudeep, S. T. S. Joseph and K. G. Thomas, *J. Am. Chem. Soc.*, 2005, **127**, 6516.
25 X. Yuan, Y. Q. Tay, X. Y. Dou, Z. T. Luo, D. T. Leong and J. P. Xie, *Anal. Chem.*, 2013, **85**, 1913.
26 M. T. Shipchandler and E. G. Moore, *Clin. Chem.*, 1995, **41**, 991.
27 P. Das, K. M. Mandal, B. N. Chandar, M. Baklya, H. B. Bhatt, B. Ganguly, S. K. Ghosh and A. Das, *Chem.–Eur. J.*, 2012, **18**, 15382.
28 X. M. Liu, N. Xi, S. J. Liu, Y. Ma, H. R. Yang, H. R. Li, J. H. He, Q. Zhao, F. Y. Li and W. Huang, *J. Mater. Chem.*, 2012, **22**, 7894.
29 Y. Ma, S. J. Liu, H. R. Yang, Y. Q. Wu, H. B. Sun, J. X. Wang, Q. Zhao, F. Y. Li and W. Huang, *J. Mater. Chem. B.*, 2013, **1**, 319.
30 P. Wang, J. Liu, X. Lv, Y. L. Liu, Y. Zhao and W. Guo, *Org. Lett.*, 2012, **14**, 520.
31 S. J. Liu, W. L. Qiao, G. Y. Cao, Y. Chen, Y. Ma, Y. Q. Huang, X. M. Liu, W. J. Xu, Q. Zhao and W. Huang, *Macromol. Rapid Commun.*, 2013, **34**, 81.
32 D. Kand, A. M. Kalle, S. J. Varma and P. Talukdar, *Chem. Commun.*, 2012, **48**, 2722.
33 Z. R. Lou, P. Li, X. F. Sun, S. Q. Yang, B. S. Wang and K. L. Han, *Chem. Commun.*, 2013, **49**, 391.
34 M. J. Wei, P. Yin, Y. M. Shen, L. L. Zhang, J. H. Deng, S. Y. Xue, H. T. Li, B. Guo, Y. Y. Zhang and S. Z. Yao, *Chem. Commun.*, 2013, **49**, 4640.
35 O. Rusin, N. N. St. Luce, R. A. Agbaria, J. O. Escobedo, S. Jiang, I. M. Warner, F. B. Dawan, K. Lian and R. M. Strongin, *J. Am. Chem. Soc.*, 2004, **126**, 438.
36 M. Zhang, M. Y. Li, Q. Zhao, F. Y. Li, D. Q. Zhang, J. P. Zhang, T. Yi and C. H. Huang, *Tetrahedron Lett.*, 2007, **48**, 2329.
37 P. Blondeau, R. Gauthier, C. Berse and D. Gravel, *Can. J. Chem.*, 1971, **49**, 3866.
38 X. F. Yang, Y. X. Guo and R. M. Strongin, *Angew. Chem., Int. Ed.*, 2011, **123**, 10878.

39 L. Yuan, W. Y. Lin and Y. E. Yang, *Chem. Commun.*, 2011, **47**, 6275.
40 J. Mei, Y. J. Wang, J. Q. Tong, J. Wang, A. J. Qin, J. Z. Sun and B. Z. Tang, *Chem.–Eur. J.*, 2013, **19**, 613.
41 J. Mei, J. Q. Tong, J. Wang, A. J. Qin, J. Z. Sun and B. Z. Tang, *J. Mater. Chem.*, 2012, **22**, 17063.
42 Z. G. Yang, N. Zhao, Y. M. Sun, F. Miao, Y. Liu, X. Liu, Y. H. Zhang, W. T. Ai, G. F. Song, X. Y. Shen, X. Q. Yu, J. Z. Sun and W.-Y. Wong, *Chem. Commun.*, 2012, **48**, 3442.
43 M. Zhang, M. X. Yu, F. Y. Li, M. W. Zhu, M. Y. Li, Y. H. Gao, L. Li, Z. Q. Liu, J. P. Zhang, D. Q. Zhang, T. Yi and C. H. Huang, *J. Am. Chem. Soc.*, 2007, **129**, 10322.
44 X. J. Zhang, X. S. Ren, Q. H. Xu, K. P. Loh and Z.-K. Chen, *Org. Lett.*, 2009, **11**, 1257.
45 A. B. Lowe, *Polym. Chem.*, 2010, **1**, 17.
46 W. H. Hao, A. McBride, S. McBride, J. P. Gao and Z. Y. Wang, *J. Mater. Chem.*, 2011, **21**, 1040.
47 S. Sreejith, K. P. Divya and A. Ajayaghosh, *Angew. Chem., Int. Ed.*, 2008, **120**, 8001.
48 Y.-K. Yang, S. Shim and J. Tae, *Chem. Commun.*, 2010, **46**, 7766.
49 A. R. Morales, C. O. Yanez, Y. Zhang, X. Wang, S. Biswas, T. Urakami, M. Komatsu and K. D. Belfield, *Biomaterials*, 2012, **33**, 8477.
50 S. K. Das, C. S. Lim, S. Y. Yang, J. H. Han and B. R. Cho, *Chem. Commun.*, 2012, **48**, 8395.
51 L. Li, J. Ge, H. Wu, Q. Xu and S. Q. Yao, *J. Am. Chem. Soc.*, 2012, **134**, 12157.
52 P. M. Ueland, H. Refsum, S. P. Stabler, M. R. Malinow, A. Andersson and H. Robert, *Clin. Chem.*, 1993, **39**, 1764.
53 T. Chung, M. Funk and D. Baker, *J. Nutr.*, 1990, **120**, 158.
54 J. Han and K. Burgess, *Chem. Rev.*, 2010, **110**, 2709.
55 F. Galindo, M. I. Buguete, L. Vigara, S. V. Luis, N. Kabir, J. Gavilovic and D. A. Russell, *Angew. Chem., Int. Ed.*, 2005, **117**, 6662.
56 M. K. Kuimova, S. W. Botchway, A. W. Parker, M. Balaz, H. A. Collins, H. L. Anderson, K. Suhling and P. R. Ogilby, *Nat. Chem.*, 2009, **1**, 69.
57 C. M. Yu, F. Zeng, M. Luo and S. Z. Wu, *Nanotechnology*, 2012, **23**, 305503.